Eur Spine J (2007) 16:701–709
DOI 10.1007/s00586-006-0263-0

ORIGINAL ARTICLE

Trunk biomechanical models based on equilibrium at a single-level violate equilibrium at other levels

N. Arjmand · A. Shirazi-Adl · M. Parnianpour

Received: 21 July 2006 / Revised: 27 September 2006 / Accepted: 30 October 2006 / Published online: 29 November 2006

Abstract Accurate estimation of muscle forces in various occupational tasks is critical for a reliable evaluation of spinal loads and subsequent assessment of risk of injury and management of back disorders. The majority of biomechanical models of multi-segmental spine estimate muscle forces and spinal loads based on the balance of net moments at a single level with no consideration for the equilibrium at remaining levels. This work aimed to quantify the extent of equilibrium violation and alterations in estimations when such models are performed at different levels. Results are compared with those of kinematics-driven model that satisfies equilibrium at all levels and EMG data. Regardless of the method used (optimization or EMG-assisted), single-level free body diagram models yielded estimations that substantially altered depending on the level considered (i.e., level dependency). Equilibrium of net moment was also grossly violated at remaining levels with the error increasing in more demanding tasks. These models may, however, be used to estimate spinal compression forces.

Keywords Single-level free body diagram model · Kinematics-driven model · Muscle forces · Equilibrium · Spine

N. Arjmand · A. Shirazi-Adl (✉)
Division of Applied Mechanics,
Department of Mechanical Engineering,
École Polytechnique, Station 'centre-ville',
PO Box 6079, H3C 3A7 Montréal, QC, Canada
e-mail: abshir@meca.polymtl.ca

M. Parnianpour
Department of Mechanical Engineering,
Sharif University of Technology, Tehran, Iran

Introduction

In manual material handling tasks and during movements involving relatively large trunk rotations, the trunk extensor muscles are at a clear mechanical disadvantage relative to the external and gravity loads when considering their respective lever arms. While counterbalancing the moment of external loads (including gravity and inertia loads), trunk extensor muscles exert forces substantially greater than external loads so much so that they could account for up to 90% of the total axial compression force acting on the spine during such activities [1, 17]. Accurate prediction of muscle forces required to maintain trunk equilibrium and stability is, hence, critical for an adequate estimation of spinal loads, and thus, for the assessment of risk of injuries in passive and active tissues. Such improvements would also benefit searches for safer lifting techniques as well as more effective prevention and treatment procedures. The infeasibility of direct quantification of muscle forces and spinal loads as well as the limitations in indirect measurement methods (e.g., intradiscal pressure measurements) have persuaded researchers towards the use of biomechanical modeling techniques.

Faced with the intricate anatomy, complex nonlinear properties and kinetic redundancy of the trunk musculoskeletal system, investigators have been obliged to make simplifying assumptions in order to estimate muscle forces and internal spinal loads. In doing so, anatomy/kinematics/passive properties/gravity loading have been simplified, nonlinearities neglected, some muscles have been overlooked or grouped as synergic sets, straight lines of action (LOA) have been assumed for trunk muscles, and finally

different cost functions or limited surface EMG data along with gain factors have been introduced. The importance of adequate representation of trunk extensor muscle anatomy [5, 14], passive properties of the ligamentous spine [3] and proper consideration of wrapping of trunk muscles in large forward flexions [4] on model predictions have been recognized.

Another major shortcoming in many current and earlier biomechanical model studies of multi-segment spinal structure lies in the consideration of the balance of net external moments only at a single cross section (typically at lowermost lumbar discs) rather than along the entire length of the spine [6, 9, 11, 14, 15, 18, 21]. This shortcoming naturally exists in dynamic and quasi-static model studies alike while simulating either sagittaly symmetric (2D) or asymmetric (3D) movements. These models have widely been employed in ergonomic applications and in injury prevention and treatment programs. It has been indicated, though with no details, that the muscle forces evaluated based on such single-level equilibrium models, once applied on the system along with external loads, may not necessarily satisfy equilibrium at remaining levels along the spine [3, 19]. The extent of violations in equilibrium at different levels and their effects on the estimated muscle forces, and spinal loads, however, have not yet been quantified.

The objective of the present study is, hence, set to quantify the extent to which the muscle/spinal loads and equilibrium requirements at various levels are influenced by results of commonly employed single-level free body diagram (SLFBD) model studies when different levels are considered. The results of our kinematics-driven (KD) model that satisfies kinematics and equilibrium requirements at all levels and directions [1, 3, 8] are used to provide input data into SLFBD models. The SLFBD model is applied separately at different disc levels (from L5–S1 to T12–L1) using the deformed configuration of the spine identical to that in the reference KD model. The violation of equilibrium at remaining levels as well as muscle forces and spinal loads are subsequently quantified and compared with each other and with the results of KD model. In order to examine the likely effect of posture and activity heaviness on results, two different isometric lifting tasks are analyzed; one in upright standing and another in forward flexed posture of 65° while holding symmetrically in both cases a 180 N load in hands. Since the net external moments, lever arm of muscles, and number of muscles that cross each spinal level change from a level to another, it is hypothesized that SLFBD models grossly violate equilibrium at remaining levels and that the estimated muscle forces and spinal loads would alter depending on the level considered (i.e., level dependency) and the posture (task) simulated.

Method

Kinematics-driven (KD) model

For the reference cases, the nonlinear finite element model along with the KD algorithm were employed to resolve redundancy in load distribution while satisfying equilibrium and kinematics conditions at all spinal levels and directions. The details of in vivo data measurements and their model studies have been described elsewhere [1, 3, 8]. In brief, a sagittaly-symmetric T1–S1 beam-rigid body model consisting of six deformable beams with nonlinear properties to represent T12–S1 segments and seven rigid elements to represent T1–T12 (as a single body) and lumbosacral vertebrae (L1–S1) is used along with 46 local and 10 global muscle fascicles having straight LOAs initially in neutral standing posture (Fig. 1). To simulate curved paths in

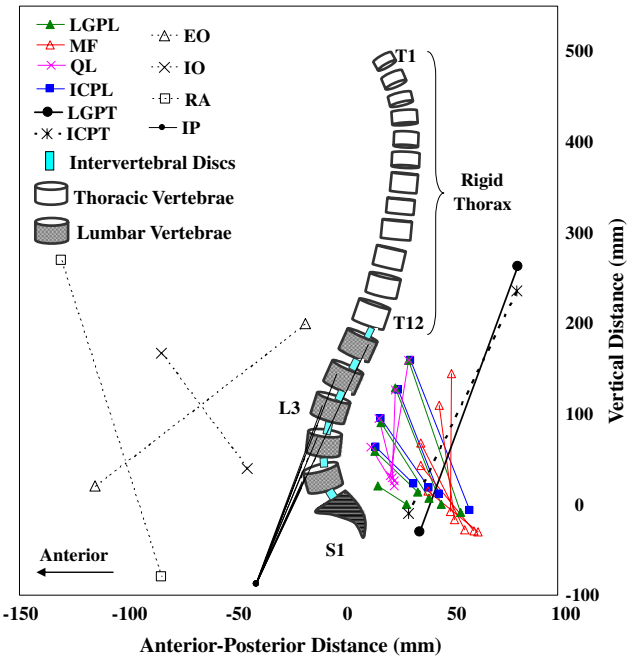

Fig. 1 The FE model as well as global and local musculatures in the sagittal plane (only fascicles on one side are shown) in upright standing posture at initial undeformed configuration. *ICPL* iliocostalis lumborum pars lumborum, *ICPT* iliocostalis lumborum pars thoracic, *LGPL* longissimus thoracis pars lumborum, *LGPT* longissimus thoracis pars thoracic, *MF* multifidus, *QL* quadratus lumborum, *IP* iliopsoas, *IO* internal oblique, *EO* external oblique and *RA* rectus abdominus (axes are not to the same scale)

forward flexion tasks, global extensor muscles are assumed to wrap around vertebrae. The wrapping contact at each T12–L5 level occurs only when the instantaneous lever arm distance at that level decreases below 10% of its corresponding value in the neutral standing posture [4]. In both cases investigated, based on the mean body weight of subjects in the in vivo study and percentage of body weight at each motion segment level reported elsewhere [16, 20], a gravity load of 387°N was considered and distributed eccentrically at different levels from T1 to L5 vertebrae. The weight of 180°N was applied at the location measured in vivo via a rigid element attached to the T3 vertebra.

Mean measured rotations at pelvis and thorax obtained from our parallel in vivo studies were prescribed on the nonlinear FE model along with the gravity forces and external load carried in hands by subjects. The total lumbar rotation is calculated as the difference between preceding measured thorax and pelvis rotations and is partitioned between individual lumbar vertebrae based on earlier measurements [see Ref. 3]. Each prescribed rotation generates an equilibrium equation at its corresponding level in the form of $\Sigma r \times f = M$ where r, f and M are lever arm of muscles with respect to the vertebra to which they are attached, unknown total forces in muscles attached to the level under consideration, and reaction moment at the vertebra under prescribed rotation, respectively. To resolve the redundancy problem, optimization algorithm with the cost function of sum of cubed muscle stresses is employed along with inequality equations of unknown muscle forces remaining positive and greater than their passive force components (calculated based on muscle strain and a tension-length relationship, [7]) but smaller than the sum of maximum physiological active forces (i.e., 0.6 × physiological cross-sectional area, PCSA) and the passive force components [3]. The cost function of sum of cubed muscle stresses has been found to be appropriate in predicting results that match EMG data [2]. The value of 0.6 MPa taken for the maximum allowable stress in muscles lies in the mid-range of reported values (0.3–1.0 MPa) [14] and is adequate in simulation of forward flexion tasks [10]. Axial and horizontal components of the calculated muscle forces along with the wrapping contact forces due to contacts between muscles and vertebrae at wrapping points are fed back onto the FE model as updated external loads and the iteration is repeated till the convergence is reach, i.e., the calculated muscle forces remain almost identical in two successive iterations. This method satisfies equilibrium at all levels and directions while accounting for the nonlinear passive stiffness of the ligamentous spine under prescribed deformed geometry of the spine that is based on in vivo measurements.

Single-level free body diagram (SLFBD) models

Under the final deformed configurations of the ligamentous spine, local and global wrapping muscles as well as gravity/external load magnitudes/locations identical to those in foregoing reference KD cases, muscle forces were re-calculated based on SLFBD equilibrium at different (L5–S1 through T12–L1) intervertebral disc mid-planes (see Fig. 2 as an example for the L5–S1 level under trunk flexion of 65°) expressed as follows:

$$\sum_{i=1}^{n} r_i \times f_i = M_{\text{ext}} - M_{\text{passive}}$$

in which n, M_{ext}, and M_{Passive} denote the number of all muscle fascicles crossing the cutting plane under consideration, the total net external moment due to gravity and external load carried in hands, and passive ligamentous resistant moment at that level, respectively. The passive ligamentous moments at different levels were taken exactly as those calculated in the reference KD models at the final deformed configurations. Unknown muscle forces were subsequently evaluated by

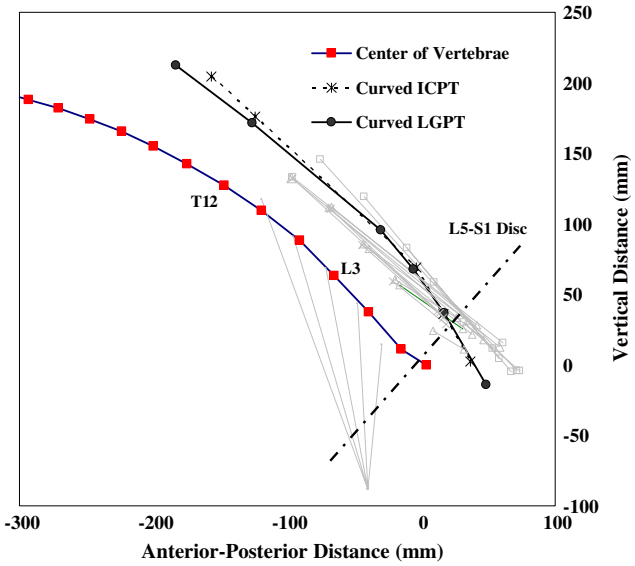

Fig. 2 Deformed configuration of the spine and the global muscles (longissimus thoracis pars thoracic, *LGPT* and iliocostalis lumborum pars thoracic, *ICPT*) with curved lines of action under flexion of 65°. The cutting transverse plane for the single-level free body diagram (*SLFBD*) model at the L5–S1 disc level is also depicted (abdominal muscles are not shown and local muscles are shown in *light gray color* for clarity of the figure)

the same optimization algorithm used in the reference models (i.e., sum of cubed muscle stresses). Spinal compression and shear forces at different levels were then computed by consideration of equilibrium in local axial and shear directions.

In order to examine whether or not the muscle forces estimated based on the SLFBD model at the L5–S1 level verify the equilibrium at remaining levels, the calculated muscle forces at this level were applied onto the FBDs at each of remaining L4–L5 through T12–L1 levels. An index of equilibrium violation (IEV), defined below, was subsequently computed at each of these levels:

$$\text{IEV } \% = \frac{(M_{\text{muscles}} + M_{\text{passive}}) - M_{\text{ext}}}{M_{\text{ext}}} \times 100$$

in which M_{muscle}, M_{Passive} and M_{ext} denote moments at the disc level under consideration generated by muscle forces calculated based on SLFBD equilibrium at the L5–S1 level, the passive ligamentous spine, and gravity/external load carried in hands, respectively. This index, IEV, represents, hence, an indication of the extent of violation in equilibrium of sagittal moment at different levels when applying the muscle forces estimated at the L5–S1 level.

Furthermore, based on the same muscle forces, axial compression force at the upper T12–L5 levels were also computed and compared at each level with their respective value estimated based directly on the SLFBD performed at that level itself rather than at the L5–S1 level. In this case, the index of error signifies the relative difference between the estimated axial compression at each level when SLFBD model is performed either at the distal L5–S1 level or at that particular level itself. It is to be re-iterated that the geometry of the spine and muscles for both loading cases used in the SLFBD models is taken identical to that in the final deformation of corresponding reference cases evaluated based on the KD models.

In order to investigate the relative effect of optimization cost function used in SLFBD models on predictions, the forward flexed task was also reanalyzed using the sum of either squared or linear muscle stresses instead of the sum of cubed muscle stresses. In this manner, muscle forces at the L5–S1 level were computed using either of these cost functions and the indices of error in equilibrium of moments (IEV) at upper levels (L4–L5 to T12–L1) were recalculated.

Finally, for the task of upright standing posture with load in hands, the muscle forces were estimated by the SLFBD performed at the L5–S1 level using the EMG-assisted approach instead of an optimization algorithm [12, 13]. For this purpose, our measured normalized EMG data under the same task and loading were considered to drive the model [8]. The normalized EMG activity in each abdominal muscle (Rectus abdominus, External oblique and Internal oblique) was taken the same and varied from 12% (as measured) to 5% or 0% while the activity in local longissimus and iliocostalis lumbar muscles was assumed the same as that measured in the multifidus (30%). The activity in quadratus lumborum (not measured in vivo) was taken half of this latter value. The activity of global longissimus and iliocostalis were taken as 30% and 24%, respectively, according to our in vivo measurements. The violation of equilibrium (IEV) was subsequently, calculated at other levels.

Results

Except otherwise specified, results are obtained using the optimization-based approach with the cost function of sum of cubed muscle stresses. For the same spinal configuration, gravity/external load magnitudes/locations and passive ligamentous resistant moment as those used in the reference KD models, muscle forces at both global and local levels substantially altered when calculated based on SLFBD model applied at different levels and that regardless of the task considered (Table 1, Fig. 3). Results indicate greater global thoracic muscle forces whereas generally smaller local lumbar muscle forces when comparing SLFBD models to KD reference cases. The differences in estimated forces in global muscles for the lifting task with 65° flexed posture further increased as the SLFBD equilibrium was considered at more distal lumbar levels reaching maximum relative values of 66% in the longissimus thoracis pars thoracic and 57% in the iliocostalis lumborum pars thoracic muscles when the SLFBD was performed at the lowermost L5–S1 level (Table 1). In accordance with the constraint requirements in KD model, many local muscles in the forward flexed lifting task were assigned lower-bound forces based on the muscle passive resistant force–length relationship and muscle instantaneous length (Table 1, underlined bold).

Local compression and shear forces at different spinal levels were also influenced when calculated based on SLFBD models; the former being smaller in both lifting tasks by as much as 9% compared with the reference KD results (Table 2). In lifting with 65° forward flexion, the local shear force at the critical L5–S1 level, however, substantially increased by 22.4%

Table 1 Predicted muscle forces under both loading cases using KD approach as well as SLFBD models at different disc levels from L5–S1 through T12–L1 (forces in Iliopsoas muscles are zero in all SLFBD models and are not shown for the KD model)

Muscle	Upper attach.	Muscle forces on each side (N)—forward flexed posture						
		KD model	Single-level free body diagram (SLFBD) model					
			L5–S1	L4–L5	L3–L4	L2–L3	L1–L2	T12–L1
LGPT	Thorax	402	668	624	521	478	444	405
ICPT	Thorax	168	264	248	187	169	169	169
LGPL	L1	26	**15**[a]	**15**	**15**	**15**	**15**	–
	L2	25	16	**16**	**16**	**16**	–	–
	L3	25	19	**18**	**18**	–	–	–
	L4	38	21	**17**	–	–	–	–
	L5	43	18	–	–	–	–	–
ICPL	L1	42	**25**	**25**	**25**	**25**	**25**	–
	L2	56	40	**39**	**39**	**39**	–	–
	L3	60	50	**42**	**42**	–	–	–
	L4	87	51	**36**	–	–	–	–
MF	L1	47	**34**	**34**	**34**	**34**	**34**	–
	L2	62	**43**	**43**	**43**	**43**	–	–
	L3	98	65	**49**	**49**	–	–	–
	L4	110	54	37	–	–	–	–
	L5	75	31	–	–	–	–	–
QL	L1	31	14	**10**	**10**	**10**	**10**	–
	L2	21	12	**11**	**11**	**11**	–	–
	L3	16	11	**10**	**10**	–	–	–
	L4	19	9	**9**	–	–	–	–
		Muscle Forces on Each Side (N) - Upright Standing Posture						
LGPT	Thorax	161	189	190	191	197	199	162
ICPT	Thorax	68	72	74	76	80	82	68
LGPL	L1	15	4	4	4	3	3	–
	L2	1	5	4	4	4	–	–
	L3	2	6	5	4	–	–	–
	L4	6	6	5	–	–	–	–
	L5	14	5	–	–	–	–	–
ICPL	L1	25	7	6	6	6	5	–
	L2	3	11	10	9	8	–	–
	L3	5	13	12	10	–	–	–
	L4	13	13	10	–	–	–	–
MF	L1	27	6	5	5	5	5	–
	L2	3	9	9	9	9	–	–
	L3	7	17	16	14	–	–	–
	L4	17	14	12	–	–	–	–
	L5	24	8	–	–	–	–	–
QL	L1	18	3	3	3	3	3	–
	L2	1	3	3	3	3	–	–
	L3	1	3	3	2	–	–	–
	L4	3	3	2	–	–	–	–

[a] Bold underlined forces indicate the constrained lower-bound in muscle forces based on passive force-length relationship and muscle instantaneous length

compared to the reference case when the SLFBD was performed at this level.

When comparing the results of SLFBD models against each other, there was a marked alteration in estimated muscle forces depending on the level considered (Table 1, Fig. 3). Furthermore, when applying the muscle forces initially estimated by the SLFBD at the L5–S1 level as known forces onto the SLFBD at remaining levels, the equilibrium of sagittal moment was found to be grossly violated. The extent of error in maintenance of equilibrium, identified as the index of equilibrium violation (IEV), increased as higher proximal levels were considered for this purpose and reached maximum values of 40% and 8% for the cut at the T12–L1 level under flexed and upright postures, respectively (Fig. 4). Similarly, axial compression forces at different levels altered substantially by as much as 51% when calculated based on SLFBD models performed either at that level itself or at the L5–S1 level (Fig. 5).

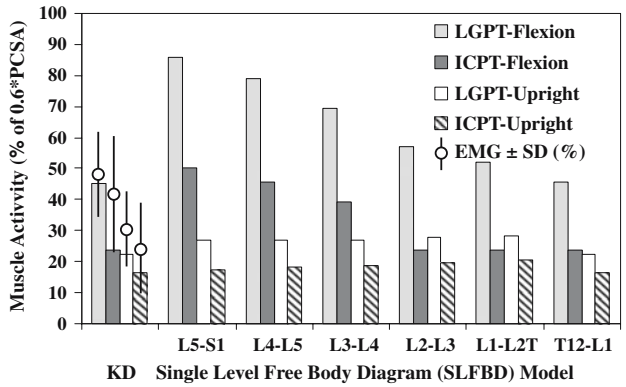

Fig. 3 Normalized (to 0.6 times physiological cross sectional area) activity of global muscles (longissimus thoracis pars thoracic, *LGPT* and iliocostalis lumborum pars thoracic, *ICPT*) for both loading cases predicted using kinematics-driven (*KD*) approach and single-level free body diagram (*SLFBD*) models considered at different T12–L1 through L5–S1 levels. Normalized (to the MVC) in vivo measured EMG activity (mean ± SD) of these muscles is also shown

When cost functions of sum of squared and linear muscle stresses were used to partition moment of L5–S1 level among muscles, the violation of equilibrium at upper levels exacerbated (see Fig. 4). In order to satisfy equilibrium at the L5–S1 level, the EMG-assisted approach predicted gain factors of 0.36, 0.52 and 1.32 MPa when no coactivity, coactivity of 5% and 12% were considered for abdominal muscles, respectively. Moment equilibrium (IEV) was violated at L4–L5 through T12–L1 levels by 5.2, 12.5, 23.9, 32.5 and 24.8%, respectively, when no coactivation was considered in abdominals. These errors further increased in presence of abdominal coactivities. To simultaneously satisfy moments at different levels, one would need to alter gains for the same muscles from a level to another a remedy that would not make much sense.

Discussion

This work aimed to quantify the extent to which the muscle forces, spinal loads and equilibrium requirements at different levels are influenced when considering single-level free body diagram (SLFBD) equilibrium at a specific spinal level or as it alters from a level to another. Such models, driven either by optimization cost functions or by EMG data, are widely employed in biomechanical model investigations of the human spine in order to estimate muscle forces and spinal loads [6, 9, 11, 14, 15, 18, 21]. For this purpose, the results of kinematics-driven (KD) model based on in vivo measurements of two lifting tasks at upright and forward flexion postures were used both to provide input data and as reference values to compare with those obtained by single-level cuts at different spinal levels. The emphasis in this work was on the reliability of SLFBD model predictions. The KD model was primarily performed to obtain deformed configurations, external/gravity load magnitudes/posi-

Table 2 Predicted local spinal loads in both loading cases using KD model as well as SLFBD models cut at different disc levels from L5–S1 through T12–L1

Disc level	Spinal loads (N)—forward flexed posture													
	KD model		Single-level free body diagram (SLFBD) model											
			L5–S1		L4–L5		L3–L4		L2–L3		L1–L2		T12–L1	
	C[a]	S[b]	C	S	C	S	C	S	C	S	C	S	C	S
T12–L1	1398	488	–	–	–	–	–	–	–	–	–	–	1407	489
L1–L2	1804	450	–	–	–	–	–	–	–	–	1699	404	–	–
L2–L3	2182	236	–	–	–	–	–	–	2028	200	–	–	–	–
L3–L4	2592	394	–	–	–	–	2402	389	–	–	–	–	–	–
L4–L5	3116	264	–	–	2958	404	–	–	–	–	–	–	–	–
L5–S1	3247	869	3172	1064	–	–	–	–	–	–	–	–	–	–
	Spinal Loads (N) - Upright Standing Posture													
T12–L1	925	–49	–	–	–	–	–	–	–	–	–	–	925	–49
L1–L2	1177	–111	–	–	–	–	–	–	–	–	1075	–93	–	–
L2–L3	1207	–157	–	–	–	–	–	–	1126	–143	–	–	–	–
L3–L4	1263	18	–	–	–	–	1197	10	–	–	–	–	–	–
L4–L5	1344	131	–	–	1268	118	–	–	–	–	–	–	–	–
L5–S1	1338	523	1244	492	–	–	–	–	–	–	–	–	–	–

[a] C: local axial compression (N)

[b] S: local shear force (N), positive in anterior direction

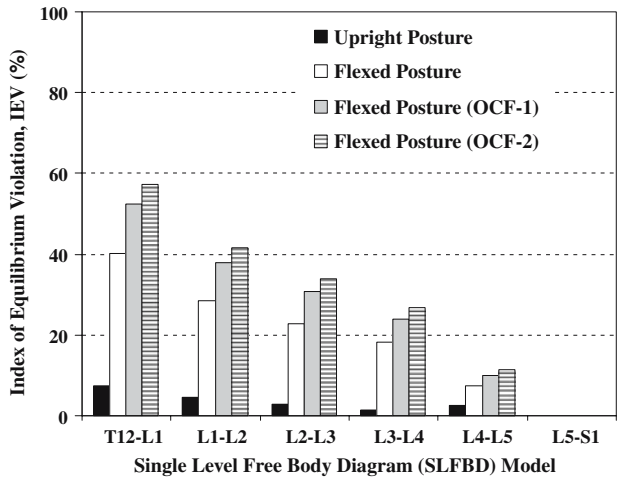

Fig. 4 Index of equilibrium violation (IEV %) at different T12–L1 through L5–S1 levels when applying muscle forces calculated based on single-level free body diagram (*SLFBD*) model at the L5–S1 level. OCF-1 and 2 refer to optimization cost functions of sum of squared and linear muscle stresses, respectively, used to partition net moment at the L5–S1 level between muscles

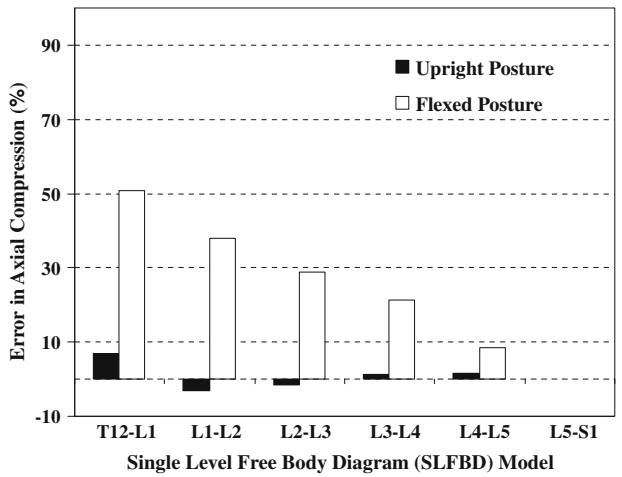

Fig. 5 Relative error in axial compression forces estimated at different spinal levels when applying the muscle forces calculated by the single-level free body diagram (*SLFBD*) model at the L5–S1 level compared to those calculated using SLFBD models directly at the level under consideration

tions, and passive resistant loads required in SLFBD models. Results of this investigation confirmed the hypotheses of the study in that SLFBD models yield results that grossly violate the equilibrium at levels other than the one considered in the model and that the extent of such violations as well as the magnitude of muscle forces and spinal loads alter as a function of disc level considered and task (i.e., task dependency) simulated. Results also demonstrated that the predictions of SLFBD models are markedly level dependent (i.e., level dependency); that is they significantly alter as a different level is used for the sake of calculation of muscle forces and internal loads.

In the KD model, the optimization algorithm was employed at all levels separately one from another in order to partition the required moment calculated for a given prescribed rotation in between muscles that are attached only to the level under consideration. The remaining muscles not attached to this specific level, either crossing over or attached to lower ones, would therefore be absent in equilibrium equations under investigation. Consideration of all levels, one by one, would therefore yield all unknown muscle forces under given kinematics and external/gravity loads. On the contrary in the SLFBD model, the forces in all muscles passing through the cross-section in question, inserted or not into that specific level, were treated as the unknowns in a single equation of equilibrium. For this reason and since identical data were shared, almost the same results were obtained in both reference and single-level models for global extensor muscle forces and local spinal loads at the T12–L1 level when the FBD was considered at the T12–L1 level (Tables 1, 2; Fig. 3). Substantial differences in global muscle forces, especially for the forward flexion task, were however found when the lower levels were considered in SLFBD model.

The SLFBD model at the lowermost L5–S1 level dealt with all global and local muscle forces as unknowns in one single equation. The optimization algorithm at this level resulted in allocation of much greater forces in global muscles due to their relatively larger PCSAs than in local muscles as compared with the muscle forces computed in KD model (Table 1, Fig. 3). For the SLFBD cut at the L5–S1 disc level and under forward flexed lifting task, global longissimus muscle activation in the optimization procedure reached 86% of its maximum force-carrying capacity (Fig. 3). Similarly, very large values of 79 and 69% were computed for the global longissimus muscle when the SLFBD was performed at the upper L4–L5 and L3–L4 levels, respectively (Fig. 3). The KD model, on the other hand, resulted in larger forces in local muscles and, hence, a more uniform partitioning of the external moment among local and global trunk extensor muscles.

Muscle forces calculated at a level, irrespective of the method used, must satisfy equilibrium when applied at remaining levels in order to be reliable. The index of violation in moment equation of equilibrium at different levels (Fig. 4) indicating the error in estimated muscle forces based on the SLFBD at the L5–S1 level increased proximally from the L5–S1 level to its maximum values of 8 and 40% at the

T12–L1 level for the upright and forward flexed lifting postures, respectively. These errors clearly lend support to the fact that equilibrium equations at all levels and directions should be treated simultaneously as are done in KD finite element model and not in isolation one from the rest as done in SLFBD models. The substantial differences between muscle forces when calculated based on the SLFBD at different levels (Table 1 and Fig. 3) also suggest the major shortcoming in such model studies. It should be re-iterated that large differences predicted in this study between the results of SLFBD models both among themselves depending on the level considered and with KD results occurred despite the use of identical deformed configurations (ligamentous spine and muscles), external/gravity magnitudes/locations, passive resistant moment of the ligamentous spine, passive properties of muscles, and optimization algorithm of sum of cubed muscle stresses. It is evident that had the muscle forces estimated from different SLFBD models been applied as additional external loads on the spine, substantially different deformed (and possibly unstable) configurations would have been generated depending on the level considered in the SLFBD. The resulting spinal configurations would also be quite different from the initial configuration considered in SLFBD calculations.

Comparison of results of SLFBD models among themselves for two lifting tasks suggests that the differences increased as a function of task demand associated with the trunk forward flexion angle. In fact, the larger the net moment of external/gravity loads becomes the greater differences (Fig. 3) and errors in equilibrium (Figs. 4, 5) one should expect from SLFBD models. That is why, the indices of error in moment equilibrium (Fig. 4) and in axial compression (Fig. 5) substantially increased when the task became physically more demanding under forward flexion lifting. Such differences are expected to exist also in dynamic lifting tasks as well as those involving asymmetry in movements (e.g., asymmetric lifts). It can, hence, be argued that the heavier and more physically demanding tasks would further deteriorate the results of SLFBD models.

Regardless of the method used to resolve the redundancy problem and partition the net moment among muscles, i.e. optimization methods or EMG-assisted approach, the equilibrium was not satisfied simultaneously at levels other than the one used to estimate muscle forces. These findings further confirm the hypothesis made in this study on the shortcoming of SLFBD models. Comparison of predicted results of KD model with SLFBD models regardless of the method used to tackle the redundancy also demonstrated that the differences in computed axial compression force at different levels remained $< 9\%$ (Table 2) being much lower than those for shear forces and muscle forces. In other words, the axial compression force appears to be less sensitive to the shortcomings in SLFBD models. Earlier investigations have also found that the effect of different optimization cost functions (especially nonlinear ones) on the estimated axial compression in both KD models [2] and SLFBD ones [15] is not significant. For this reason and due to the relative ease in SLFBD applications, one may argue that such SLFBD models could be carried out with the specific objective to estimate only local compression loads on the spine but not the shear forces and muscle activation levels.

Acknowledgment This research is supported by a grant from the Natural Sciences and Engineering Research Council of Canada, NSERC.

References

1. Arjmand N, Shirazi-Adl A (2005) Biomechanics of lumbar posture in static lifting tasks. Spine 30:2637–2648
2. Arjmand N, Shirazi-Adl A (2006a) Sensitivity of kinematics-based model predictions to optimization criteria in static lifting tasks. Med Eng Phys 28:504–514
3. Arjmand N, Shirazi-Adl A (2006b) Model and in vivo studies on human trunk load partitioning and stability in isometric forward flexions. J Biomech 39:510–521
4. Arjmand N, Shirazi-Adl A, Bazrgari B (2006c) Wrapping of trunk thoracic extensor muscles influences muscle forces and spinal loads in lifting tasks. Clin Biomech 21:668–675
5. Bogduk N, Macintosh JE, Pearcy MJ (1992) A universal model of the lumbar back muscles in the upright position. Spine 17:897–913
6. Cholewicki J, McGill SM, Norman RW (1995) Comparison of muscle forces and joint load from an optimization and EMG assisted lumbar spine model: towards development of a hybrid approach. J Biomech 28:321–331
7. Davis J, Kaufman KR, Lieber RL (2003) Correlation between active and passive isometric force and intramuscular pressure in the isolated rabbit tibialis anterior muscle. J Biomech 36:505–512
8. El-Rich M, Shirazi-Adl A, Arjmand N (2004) Muscle activity, internal loads and stability of the human spine in standing postures: combined model-in vivo studies. Spine 29:2633–2642
9. Granata KP, Lee PE, Franklin TC (2005) Co-contraction recruitment and spinal load during isometric trunk flexion and extension. Clin Biomech 20:1029–1037
10. Guzik DC, Keller TS, Szpalski M, Park JH, Spengler DM (1996) A biomechanical model of the lumbar spine during upright isometric flexion, extension and lateral bending. Spine 21:427–433
11. Marras WS, Parakkat J, Chany AM, Yang G, Burr D, Lavender SA (2005) Spine loading as a function of lift frequency, exposure duration and work experience. Clin Biomech 21:345–352

12. Marras WS, Granata KP (1997) The development of an EMG-assisted model to assess spine loading during whole-body free-dynamic lifting. J Electromyogr Kinesiol 7:259–268
13. McGill SM (1992) A myoelectrically based dynamic three-dimensional model to predict loads on lumbar spine tissues during lateral bending. J Biomech 25:395–414
14. McGill SM, Norman RW (1986) Partitioning of the L4–L5 dynamic moment into disc, ligamentous and muscular components during lifting. Spine 11:666–678
15. Parnianpour M, Wang JL, Shirazi-Adl A, Sparto P, Wilke HJ (1997) The effect of variations in trunk models in predicting muscle strength and spinal loads. J Musculoskelet Res 1:55–69
16. Pearsall DJ (1994) Segmental inertial properties of the human trunk as determined from computer tomography and magnetic resonance imagery. PhD thesis, Queen's University, Kingston, Ontario
17. Reeves NP, Cholewicki J (2003) Modeling the human lumbar spine for assessing spinal loads, stability and risk of injury. Crit Rev Biomed Eng 31:73–139
18. Schultz AB, Andersson GB, Haderspeck K, Ortengren R, Nordin M, Bjork R (1982) Analysis and measurement of lumbar trunk loads in tasks involving bends and twists. J Biomech 15:669–675
19. Stokes IA, Gardner-Morse M (1995) Lumbar spine maximum efforts and muscle recruitment patterns predicted by a model with multijoint muscles and joints with stiffness. J Biomech 28:173–186
20. Takashima ST, Singh SP, Haderspeck KA, Schultz AB (1979) A model for semi-quantitative studies of muscle actions. J Biomech 12:929–939
21. van Dieen JH, Kingma I, Van der Bug P (2003) Evidence for a role of antagonistic cocontraction in controlling trunk stiffness during lifting. J Biomech 36:1829–1836